Vibration Analysis of a Rotary Compressor

Hyung-Suk Han[1,#], Seon-Woong Hwang[2] and Jeong-Seo Koo[3]

[1] New Transportation System Group, Korea Institute of Machinery & Materials (KIMM), Daejeon, Republic of Korea
[2] Air Conditioning Compressor Division, LG Electronics, Changwon, Republic of Korea
[3] Korea Railroad Research Institute, Uiwang- City, Kyungido, Republic of Korea

ABSTRACT

The vibration of a rolling piston type rotary compressor for air-conditioning use is analyzed numerically and experimentally. Multibody dynamic analysis methods to predict the vibration are given. The compressor is modeled as a multibody system composed of bodies, joints, and force elements. Experimental results are shown to compare with simulation results. A sensitivity study using different variables that affect the compressor vibration is also carried out. It is found that the mass of the weight balancer plays an important role in acceleration.

Key Words : Rotary compressor, Vibration analysis, Multibody dynamics

Nomenclature

$\boldsymbol{q}$ = position
$\dot{\boldsymbol{q}}$ = velocity
$\ddot{\boldsymbol{q}}$ = acceleration
$\boldsymbol{M}$ = mass
$\boldsymbol{\Phi_q}$ = constraint jacobian
λ = lagrange multiplier
$\boldsymbol{Q}$ = generalized
γ = right side of constraint acceleration
F_g = gas compression force
T_g = gas compression torque
h = height of cylinder
P_b = suction charge pressure
P_c = compression pressure
P_s = suction pressure
P_d = discharge pressure

Manuscript received: September 8, 2003 ;
Accepted: April 20, 2004
Corresponding Author:
Email: hshan@kimm.re.kr
Tel: +82-42-868-7814, Fax: +82-42-868-7844

1. Introduction

A rotary-type compressor that uses a rolling piston as its compression mechanism is being widely used in air conditioners and refrigerators. When compared with the reciprocating compressor, the rotary-type compressor has a higher performance and is cheaper, smaller, and lighter. However, in terms of vibration, there exist cases when the rotary-type compressor has disadvantages in comparison with the reciprocating compressor because of the different suspension systems used. Generally, isolation is done in two stages in the reciprocating compressor. The first stage involves the coil spring that supports the motor in the inner parts of the case. The second stage involves an exterior isolator which supports the case at the base mainly by using rubber mounts. On the other hand, the excited vibration in the rotary-type compressor is relatively small. So the first stage, an inner isolating device, does not exist in the rotary-type compressor. Instead, the rotary-type compressor is supported solely by the second stage, an exterior isolator, making it relatively more difficult to control the vibration. The reduction of vibration is an important factor to consider in the design of compressors. Because of the trend of customers wanting high quality and the fact that

many frame buildings exist in many countries, it can be said that the reduction of vibration in compressors is an important factor for expansion into international business fields. Not much research has been done in the prediction and reduction of vibration in rotary-type compressors in comparison with reciprocating compressors. In the prediction of vibration obtained by using transient dynamic analysis of the rotary-type compressor, research has been done mainly by using an analysis model of a simplified compressor[1-4]. Once a vibration analysis program is developed, its advantages can easily be put to practical use. However, if the configuration of the compressor is altered, additional research has to be done on the analysis model based on the alteration.

In the present paper, the application of the multibody dynamics to the rotary-type compressor is shown. The advantage of multibody dynamics is that, at the present, modeling closest to the physical system can be done for the dynamic modeling of multibody systems. Therefore, all the components, constraints, and the driving conditions can be considered in detail. Furthermore, the body can be modeled into a flexible body, and so the elastic deflection can be considered as well. In the present paper, multibody dynamics was used to construct an analysis model of the rotary-type compressor and accelerations were predicted numerically. We performed experimentations for the validation of the analysis model and compared the accelerations. By using the results, we investigated the weight balancer used for the balance of the imbalance of mass, the stiffness of the isolator, and the inertia of case to study the sensitivity of the vibration. Then we present the direction of design based on the investigations. As a result, the validity of the application of multibody dynamics theory to the rotary-type compressor can be shown.

2. Multibody Dynamics

Fig. 1 shows a multibody system. This system is composed of nb rigid bodies, and a coordinate of $6 \times nb$ is needed to represent the motion in the space. This kind of generalized coordinate, however, is not all independent because of the joints between adjacent bodies. The motion of each body is affected by kinematic constraints which define the generalized coordinate and the velocity relationship of the generalized coordinate. In order to control and understand motion within the multibody system, bodies, joints, and the force element need to be defined. If there is a system composed of nb bodies, then the generalized coordinate is defined as the vector $\mathbf{q}$ below.

$$\boldsymbol{q} = \left[q_1, q_2, \ldots, q_{nb\times 6}\right]^T \tag{1}$$

If there are m constraint equations within the system, they are represented as Equation (2), and the system equations of motion of the constrained mechanical system is defined as Equation (3).

$$\boldsymbol{\Phi}(\boldsymbol{q},t) = \left[\Phi_1(\boldsymbol{q},t), .., \Phi_m(\boldsymbol{q},t)\right]^T = \mathbf{0} \tag{2}$$

$$\boldsymbol{M}\ddot{\boldsymbol{q}} + \boldsymbol{\Phi}_q{}^T \boldsymbol{\lambda} = \boldsymbol{Q} \tag{3}$$

To adequately use Equation (3), the first and second derivatives of Equation (2) are necessary.

$$\boldsymbol{\Phi}_q \dot{\boldsymbol{q}} + \boldsymbol{\Phi}_t = \mathbf{0} \tag{4}$$

$$\boldsymbol{\Phi}_q \ddot{\boldsymbol{q}} = -(\boldsymbol{\Phi}_q \dot{\boldsymbol{q}})_q \dot{\boldsymbol{q}} - 2\boldsymbol{\Phi}_{qt}\dot{\boldsymbol{q}} - \boldsymbol{\Phi}_{tt} \equiv \boldsymbol{\gamma} \tag{5}$$

By using Equation (3) and Equation (5), the system equation of motion in matrix form is defined as Equation (6).

$$\begin{bmatrix} \boldsymbol{M} & \boldsymbol{\Phi}_q{}^T \\ \boldsymbol{\Phi}_q & \mathbf{0} \end{bmatrix} \begin{Bmatrix} \ddot{\boldsymbol{q}} \\ \boldsymbol{\lambda} \end{Bmatrix} = \begin{Bmatrix} \boldsymbol{Q} \\ \boldsymbol{\gamma} \end{Bmatrix} \tag{6}$$

For the analysis of the equations of motion of this kind multibody systems, refer to the bibliography[5]. At present, general-purpose multibody dynamic analysis programs such as DADS[6], ADAMS[7], SIMPACK[8], and RecurDyn[9] are commercially available.

When the multibody dynamics analysis method is applied, there are advantages from several aspects. The multibody dynamics analysis model is closer in form to the physical system, and the model is also adaptable for applications in virtual engineering. Since it resembles the physical system, consideration of various boundary conditions within the multibody dynamics analysis model is possible, and the factors that can be investigated relatively increase in number. The multibody dynamics analysis model has the advantage of enabling

investigation of design using a virtual prototype that includes factors such as vibration analysis, sound analysis, stress analysis, and durability analysis. This can be done without the use of the actual physical system. Therefore, we can conclude that the use of multibody dynamics vibration prediction method is rational. However, there is one disadvantage of the multibody dynamics analysis model; it is more complicated in analysis modeling than using in-house programs that are based on a simplified model. We think the appropriate thing to do is to use in-house programs in the initial concept design stage where a prompt derivation of results is needed. Then in the detail design stage, the multibody dynamics analysis method should be applied. In this way, not only can experiments using the actual system be replaced, but also the investigation of factors that are difficult to measure in the experiment or difficult to change in design can be made possible by simulation.

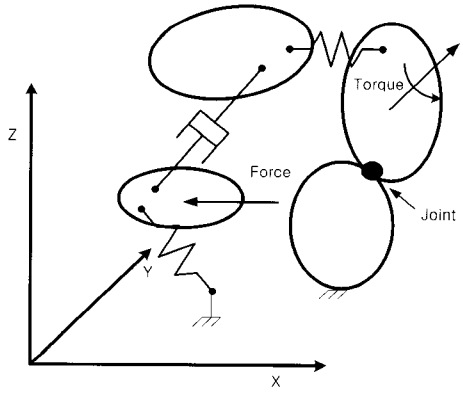

Fig. 1 Multibody system

3. Modeling

3.1 Structure of a Rotary-type Compressor

Fig. 2 shows the outline structure of a rotary-type compressor. The motor is fitted onto the upper end of the case and the compression mechanism is spot-welded onto the lower end of the case. The motor and compression mechanism is connected and rotated by the shaft. The case is supported by the isolating rubber of the base. In the compression mechanism, the rolling piston rotates within the cylinder by the rotation of the shaft. The application of suction, compression, and discharge takes places in the chamber inside the cylinder in accordance to the rotation of the rolling piston. In this type of compressor, the following factors excite the vibration: gas compression moment due to periodic changes in the repetitive refrigerant gas, fluctuation of the motor torque, the imbalance of mass in the rotating parts, the centrifugal force caused by the eccentric revolution of the rolling piston, and finally the inertia force caused by the reciprocating motion of the vane. Among these factors, the gas compression moment due to periodic changes in the gas and the fluctuation of the motor torque have been known to be the primary influences[3]. Also the tangential vibration is most important compared with vibrations in other directions. Table 1 shows the main properties of the compressor mentioned in this paper. The power of the compressor is 780 W, the discharge per one revolution is 16.4 cc, and the diameter is 112 mm.

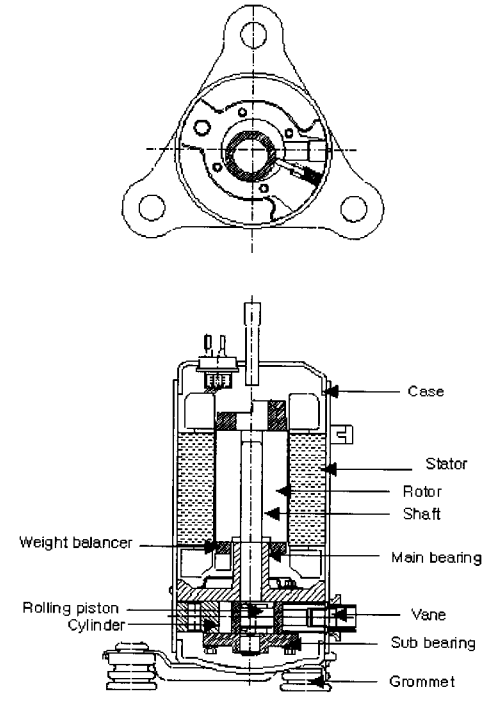

Fig. 2 Schematic view of rolling piston type rotary compressor

Table 1 Inertia and stiffness properties

Mass properties				
	Mass (kg)	Ixx (kg· m^2)	Iyy (kg· m^2)	Izz (kg· m^2)
Cylinder	0.618	2.89e-4	6.96 e-4	9.26 e-4
Main bearing	0.594	5.12 e-4	4.91 e-4	9.09 e-4
Sub bearing	0.193	0.60 e-4	0.62 e-4	1.19 e-4
Shaft	0.233	5.13 e-4	5.14 e-4	1.24 e-5
Roller	0.117	0.22 e-4	0.22 e-4	3.29 e-5
Vane	0.018	0.91 e-6	1.69 e-6	0.83 e-6
Rotor	1.200	1.22 e-3	1.22 e-3	4.99 e-4
Balance weight	0.080	1.72 e-5	4.78 e-6	1.88 e-5
Stator	4.450	1.04 e-2	1.06 e-2	8.83 e-3
Shell	1.815	1.79 e-2	1.78 e-2	5.99 e-3
Top cap	0.274	2.25 e-4	2.21 e-4	4.14 e-4
Bottom cap	0.892	1.56 e-4	1.52 e-4	2.96 e-4
accumulator	0.460	1.26 e-3	2.17 e-4	1.27 e-3

Isolator Properties	
Stiffness of radial(N/m)	9,671
Stiffness of axial(N/m)	53,740

Spring Properties	
Stiffness(N/m)	1,786
Free length	2.73e-2

3.2 Compression Mechanism

The most important and the most difficult part of the rotary-type compressor vibration analysis model is the compression mechanism. Within the compression mechanism, sliding and bearing between different parts exist, and this is how lubrication takes place. Therefore, there are difficulties in modeling the exact mechanics of the compression mechanism. Modeling of lubrication is described in Section 3.4.4 in detail. In the present paper, lubrication was considered when comparing a relatively complex analysis model with a relatively simple analysis model. The difference in the results between the two models was small, and therefore the simple analysis model was put into application. In other words, factors other than the gas compression torque, such as joint and force elements are modeled as described in Section 3.4 by using the multibody dynamics analysis method. Fig. 3 shows how the acting force caused by the refrigerant compression within the interior of the compression mechanism is simplified. F_g and T_g in Fig. 3 are defined as Equations (7) and (8).

$$F_g = 2hr(p_c - p_b)\sin\{(\theta+\alpha)/2\} \quad (7)$$

$$T_g = eF_g \sin\{(\theta+\alpha)/2\} \quad (8)$$

Here, pressure p_b within the suction chamber can be assumed to be constant. It is also assumed that the pressure p_b is equal to the compressor suction pressure p_s. The compresstion pressure, p_c increases and arrives at the value equal to the compressor discharge pressure, p_d. In the present paper, theoretical values were used for the above parameters. Fig. 4 shows the theoretical pressure change of p_c. This theoretical value is inputted by using the curve element of DADS and is used in the user-defined subroutine. Equation (7) and Equation (8) are defined by using the user-defined subroutine FRCUDF in DADS. After sensing the variables included in Equation (7) and Equation (8), FRCUDF calculates each Equation and then applies the force to each corresponding body. At the initial stages, in-house performance analysis programs of LG Electronics was performed after applying specific Equations related to lubrication. This was done for validation. However, even if only the simple Equations (7) and (8) were considered, there was a minute difference in the prediction of the gross vibration of the compressor. F_v, F_m, F_k, and F_d are modeled by general multibody dynamics elements. F_v is a vane contact force, and it is defined by the Slider-Curve element of DADS. F_m is an inertia force of the vane, and it is calculated in the Body element of DADS. F_k is a spring force, F_d is a pressure differential force on vane, and they are modeled as TSDA elements of DADS.

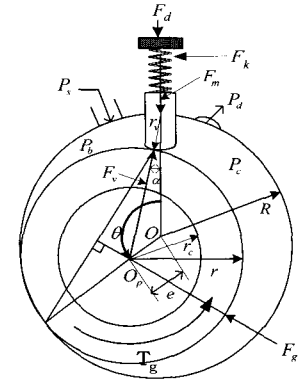

Fig. 3 Explanation of acting forces

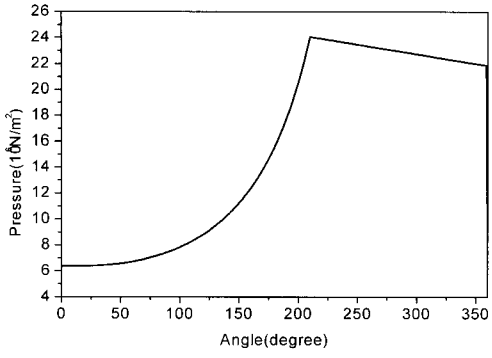

Fig. 4 Compression pressure

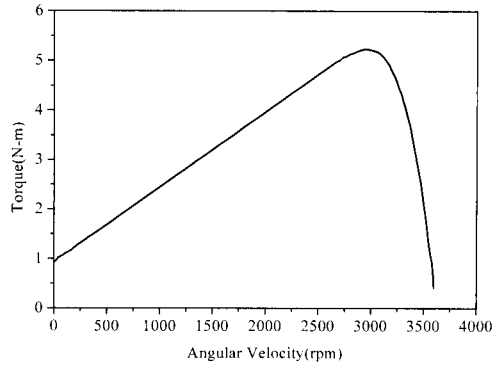

Fig. 5 Characteristics of motor

3.3 Motor

The motor performance curve is used in the dynamic modeling of the driving motor. The motor performance curve is an experimental value and is represented on the x-axis as the angular velocity(rpm), and on the y-axis as torque (Nm). Fig. 5 shows the performance curve of the motor used in the present paper. In order to use the motor torque, the rotational spring-damper (RSDA) element of DADS was used. RSDA calculates the torque by using the relative angle and the relative angular velocity between two bodies. The motor was modeled by applying the RSDA element between the shaft and the cylinder. In reality, torque is generated between the rotor and the stator. But since there is a problem of redundancy at the time of the multibody dynamics modeling, the RSDA was applied between the shaft and the cylinder. According to analysis results, there was no difference in the acceleration response between applying the RSDA between the rotor and the stator and applying it between the shaft and cylinder.

The motor torque is modeled by inputting the performance curve shown in Fig. 5 into the defined parts of the nonlinear curve for the nonlinear damper of the RSDA element. In this way, the relative rotating speed between the shaft and cylinder is detected by the RSDA element. Then the motor torque due to the rotating speed is calculated by using Fig. 5, and the calculated torque is applied to the shaft and cylinder afterwards. By using this kind of modeling method, the torque characteristic of the actual motor can be implemented by simulations. Also, the vibration prediction at the beginning and end of operation can be done by modifying the performance curve.

3.4 Body, Joint and Force Element

3.4.1 Body

The bodies considered in the analysis model are the cylinder, rolling piston, vane, rotor, stator, case, weight balancer, shaft, main bearing, sub-bearing, accumulator, top cap, and bottom cap. The mass and the center of gravity of the body were extracted from I-DEAS. The geometry of each body is taken from I-DEAS and inputted into DADS. Then the motion of the compressor is visualized.

3.4.2 Joint

The joint that composes the analysis model is shown in Table 2. Fig. 6 shows the joints used. These joints are ordinary joints used in the multibody dynamics. The particular aspect of Table 2 is that the Slider-Curve element was applied between the vane and the piston. This element is one that defines geometric contact of general profile. In this paper, the 7th order polynomial is applied as Equation (9) in order to define the profile of vane and roller.

$$\begin{aligned} x_i &= a_{0i} + a_{1i}u_i + a_{2i}u_i^{\,2} + a_{3i}u_i^{\,3} + \cdots + a_{7i}u_i^{\,7} \\ y_i &= b_{0i} + b_{1i}u_i + b_{2i}u_i^{\,2} + b_{3i}u_i^{\,3} + \cdots + b_{7i}u_i^{\,7} \end{aligned} \tag{9}$$

3.4.3 Force Element

Fig. 7 shows the force elements used in the dynamic model of a compressor. In the compressor, there exists a spring which works on the vane and cylinder. There also exist three rubber mounts in the base and the lower cap. The spring that is installed in the vane and cylinder was modeled by the translational spring-damper (TSDA) element of DADS. The stiffness of the rubber mounts

takes on nonlinear characteristics. Therefore, the force element applied by using the nonlinear characteristic curve obtained from experiments is the BUSHING element. This element takes on a six-directional stiffness and damping. The friction between vane and slot applies a friction element to the translation joint. The friction coefficient used is 0.01.

Table 2 Joints of compressor

Joint	Body i	Body j
Bracket	Case	Cylinder
Bracket	Case	Stator
Bracket	Case	Accumulator
Bracket	Case	Top cap
Bracket	Case	Bottom cap
Bracket	Cylinder	Sub bearing
Bracket	Cylinder	Main bearing
Bracket	Rotor	Weight balancer
Bracket	Rotor	Shaft
Revolute	Cylinder	Shaft
Cylindrical	Roller	Shaft
Translational	Cylinder	Vane
Slider-Cruve	Roller	Vane

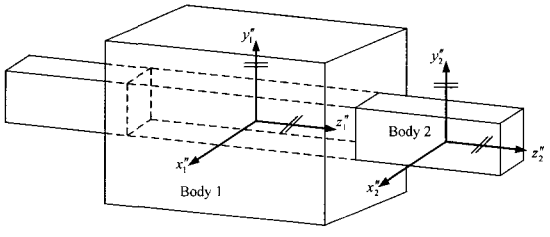

(a) Translational joint

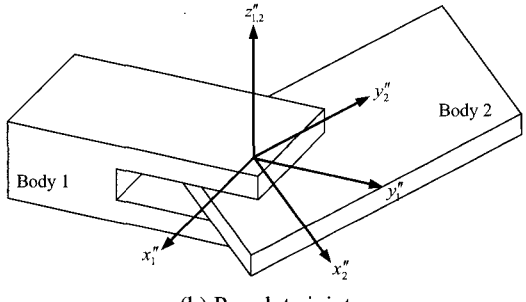

(b) Revolute joint

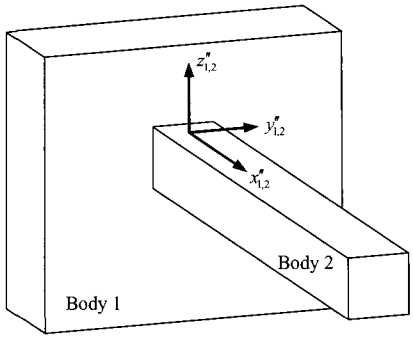

(c) Bracket joint

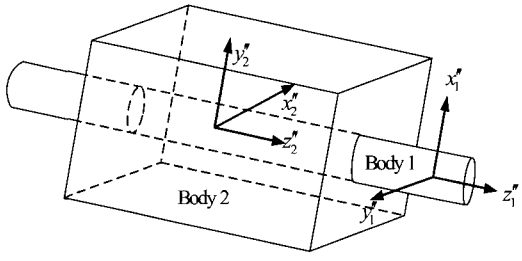

(d) Cylindrical joint

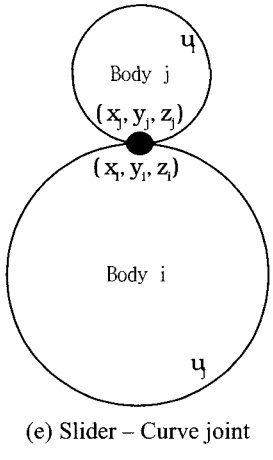

(e) Slider – Curve joint

Fig. 6 Joints used in compressor model

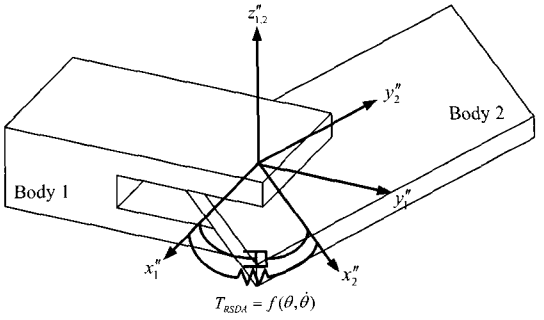

(a) RSDA element

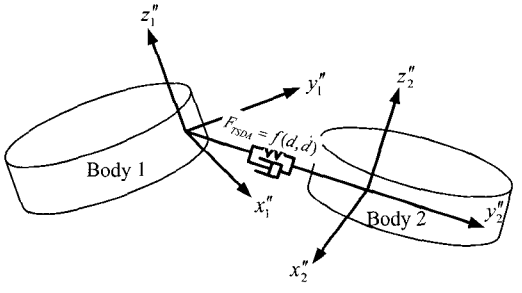

(b) TSDA element

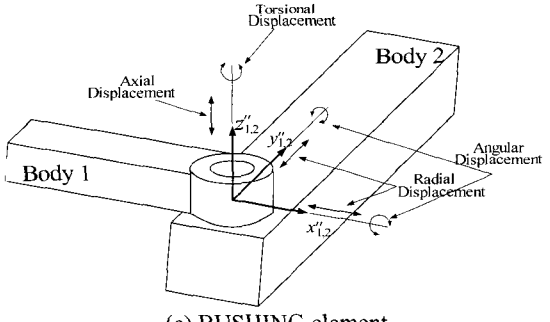

(c) BUSHING element

Fig. 7 Force elements used in compressor model

3.4.4 Lubrication

In the rotary-type compressor, sliding motion exists in various places. And in the sliding parts, lubrication is done by oil. At the initial stages, equations related to lubrication were considered by using the user-define subroutines of DADS. However, obtaining related parameters was difficult, and the effect was seemed small in literature and analysis results[3]. Therefore, one coefficient of mechanical loss was simply modeled. In other words, by using the coefficient in proportion to the angular velocity, we modeled it to work as a mechanical loss moment. The coefficient of mechanical loss was estimated using the angular velocity generated from the experiment. In other words, the coefficient of mechanical loss that makes the deviation range identical by comparing the result of angular velocity of motor and angular velocity of the experiment was estimated using trial-and-error, and the estimated coefficient of loss is 3×10^{-5} N· m· s/rad. This kind of coefficient of loss is modeled applying RSDA to the revolute joint which connects the shaft-cylinder. Fig. 8 shows DADS analysis model according to the rigid multibody dynamic model described above. Fig. 9 shows the compression mechanism.

4. Results

4.1 Experiment

To investigate the validity of the vibration analysis, we performed experiments. Fig. 10 shows the measurement point of acceleration in the experiment. The accelerometer was installed at (24.5 mm, 53.9 mm, 21.95 mm) and measured the tangential and radial accelerations. The experiment was performed after placing the compressor on the floor and letting the refrigerant gas flow by using a flexible hose. The accelerometer used in the experiment is Type 4393 of B&K company. Since the amplitude of acceleration was used in the vibration quality control of the product, the peak acceleration was measured. The peak acceleration was used in comparative validation of the experiments and simulation in this paper.

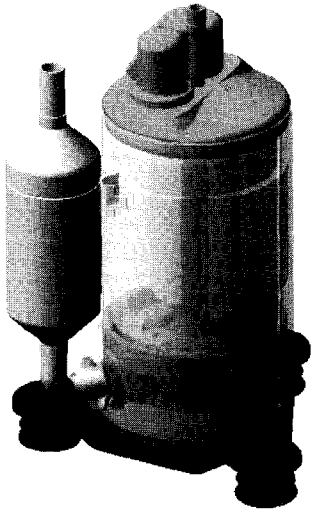

Fig. 8 DADS model of the rotary compressor

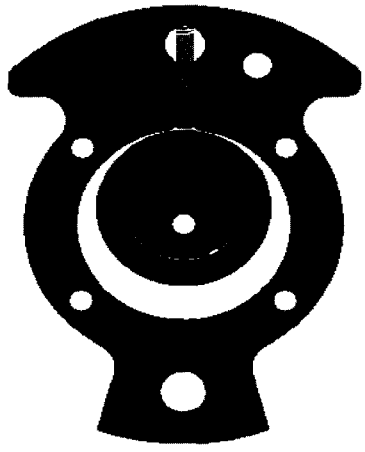

Fig. 9 DADS model of the compression mechanism

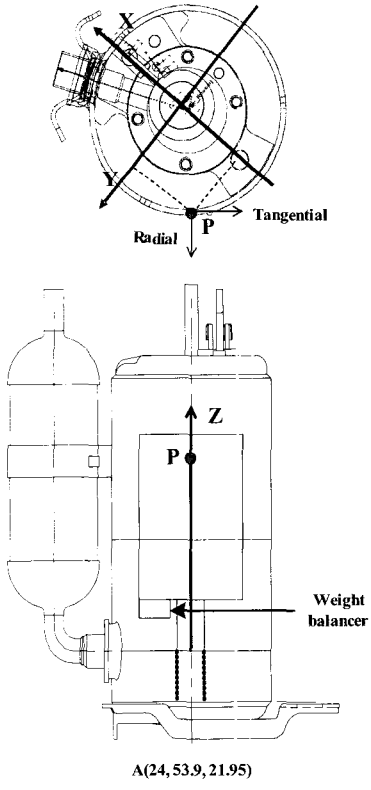

Fig. 10 Measurement point P

4.2 Simulation Results

Fig. 11 shows the tangential and radial accelerations, which resulted from the measurement point P by simulations according to time. Based on the first peak, the tangential acceleration shows 6.5 m/s^2, and the radial acceleration shows 2.7 m/s^2. In order to compare the validation of the simulation results, the results of the experiment were compared as shown in Table 3. The experiment and simulation were compared, categorizing them into compression and no compression, which means the cases with refrigerant and without refrigerant. In the tangential acceleration, the experiment had 7.0 m/s^2 which is 0.5 m/s^2 greater than the simulation result, but it shows that the difference between the experiment and simulation is small. In the radial acceleration, the experiment had 2.8 m/s^2 which also is similar to the simulation. A peculiarity here is that the tangential acceleration of the case is twice of the radial one. According to the results of Table 3, the effect of the compression mechanism with vibration can be observed. When there was no compression, the tangential acceleration of the case was reduced by 60 % in both experiment and simulation. On the other hand, the radial acceleration of the case showed no change. The acceleration of the case with no compression only occurred in the rotating parts, so it can be inferred that the weight imbalance of rotating parts caused it. The imbalance of rotating parts affected the tangential acceleration by 40 % and the radial one by 100 %. Therefore, the radial acceleration has to be controlled by the management of imbalance of the rotating parts. On the other hand, it shows that the tangential acceleration needs to be controlled by a compression mechanism with a reduction of imbalance.

Fig. 11 and Table 3 show the acceleration of simulation and experiment being similar to each other, so the reliability of the simulation model was validated. Therefore, a design-sensitivity analysis of acceleration is possible with simulation. The effect of three types of design variables and peak acceleration is analyzed in the next section.

Table 3 Comparison of accelerations (Unit: m/s^2)

Cases	Tangential		Radial	
	Test	Simulation	Test	Simulation
Compression	7.0	6.5	2.8	2.7
No compression	2.8	2.7	2.8	2.6

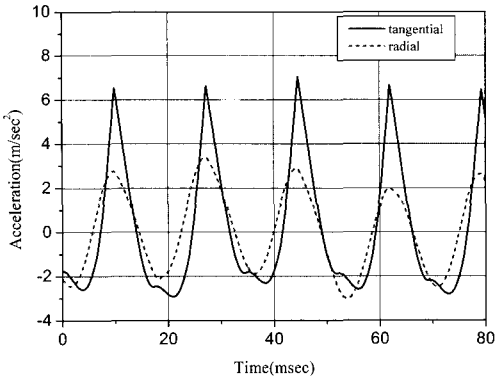

Fig. 11 Simulated accelerations on point P

4.2.1 Effect of the Weight Balancer

For the weight balancer of the compressor, two balancers were installed. In order to analyze the effect of the weight balancer attached at the bottom end of the rotor, simulation and experiments were done in four cases. The analysis and experiment were done in cases with three weight balancers of different weights and without the weight balancer. The geometry of the three weight balancers is shown in Fig. 12. The centers of gravity of the three weight balancers were made identically. The three weight balancers have an effect of moment of inertia on the rotating parts and also on weight imbalance. Fig. 13 shows the tangential acceleration at point P. As shown in Fig. 13, when the mass increased, the acceleration decreased. An increase of the moment of inertia on the z-axis of rotating parts decreased the tangential acceleration. Fig. 14 shows the radial acceleration, and it tends to have a parabolic shape. The least values were determined to be 80 g by experiment and 60 g by simulation. There is difference between the experiment and simulation results in the radial acceleration. There may be many causes, but it is thought to be the difference in mass of the simulation and model. Also the flexibility not being considered can be another cause. However, further investigation is needed. It can be also thought that the mass in the simulation is an ideal value generated from I-DEAS, and the model includes production tolerance. When generalizing Fig. 13 and Fig. 14, it can be concluded that the optimum design of the four weight balancers is in the range of 60 g~80 g. Here, the weight balance considering only static balancing is 62 g.

In both experiment and simulation, when the mass increased, the tangential acceleration decreased; but with the radial, the least values are expressed at 60 g in simulation and 80 g in experimentation. The reason for this can be the difference in the mass or effects of other unknown elements, so it is considered to increase the number of samples in the experiments to validate the statistical reliability for further study.

Fig. 12 3 different weight balancers

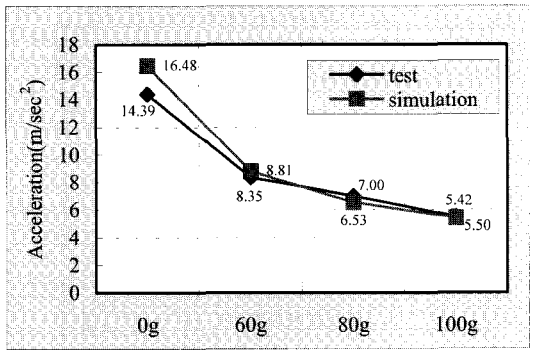

Fig. 13 Tangential accelerations as a function of the mass of weight balancer

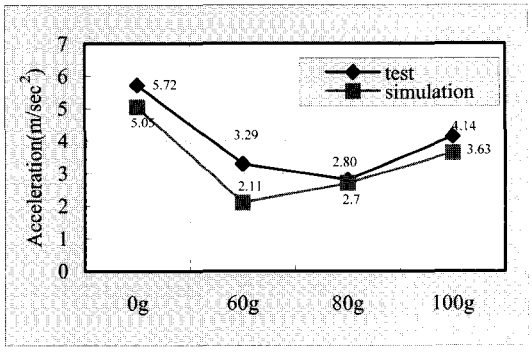

Fig. 14 Radial accelerations as a function of the mass of weight balancer

4.2.2 Effect of the Stiffness of Rubber Mounts

Three types of isolators were applied to the same compressor to be experimented and simulated. The stiffness of the isolators was found to have nonlinear

characteristics. In the simulation, nonlinear stiffness was used. Table 4 shows the stiffness in the linear section of the three types of isolators. The stiffness increased in the order of A<B<C. Fig. 15 shows results of the tangential acceleration at point P. As shown in Fig. 15, an increase of the stiffness increased the acceleration in both experiment and simulation. However, the difference is very small. When the stiffnesses of A and C were different by about three times, the change in the acceleration was less than 10 % in simulation.

Table 4 Stiffness of isolators

Model	Axial (N/m)	Radial (N/m)
A	53,740	9,671
B	123,370	20,738
C	149,278	29,000

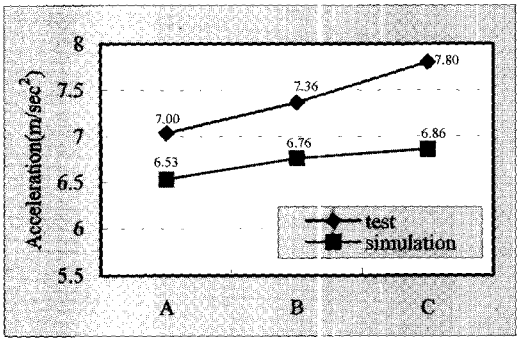

Fig. 15 Tangential accelerations as a function of the stiffness of isolators

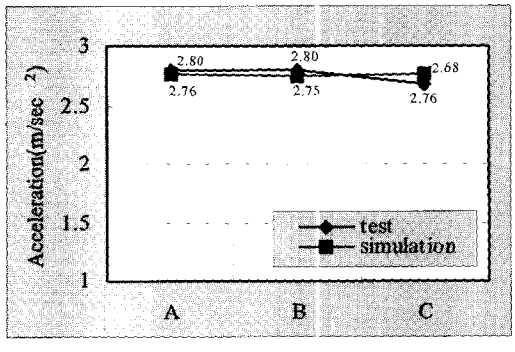

Fig. 16 Radial accelerations as a function of the stiffness of isolators

Fig. 16 shows the radial acceleration at point P. Also, with the radial acceleration, the effect on the radial acceleration was small in both experiment and simulation.

4.2.3 Effect of the Case Inertia

The effect on the acceleration was validated according to the increase of times inertia of the case. The inertia, which was increased by 1.5 and twice greater than the initial model, was simulated but not experimented. The purpose was to understand the quantity of simulation. The height of a compressor was reduced and the diameter was increased to consider the design plan that increases I_{zz} of the case. The tangential acceleration was decreased by approximately 20 % when the inertia was increased twice(Fig. 17).On the other hand, the effect on the radial acceleration was not significant(Fig. 18).

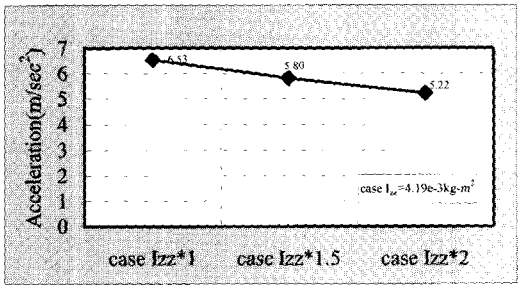

Fig. 17 Tangential accelerations as a function of the moment of inertia of case

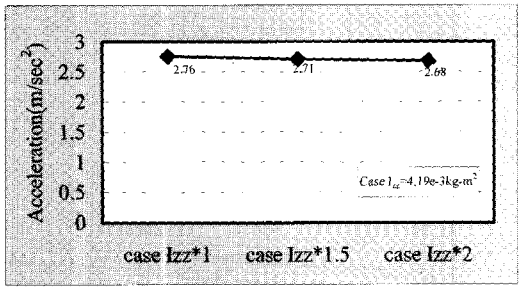

Fig. 18 Radial accelerations as a function of the moment of inertia of case

Since the case was stationary, it had less effect in terms of inertia than the rotating part. Realistically, decreasing the height of a compressor and increasing its diameter can not only increase the case I_{zz} of the case, but it has to increase the inertia of the rotating part. Therefore, it is predicted that the reduction of acceleration has greater effects on quantity than on the inertia of case.

4. Conclusion

In the present paper, the prediction of vibration of the rolling piston type rotary compressor was introduced. Through the research, the following conclusions were obtained.

(1) We confirmed that the multibody dynamics analysis method could be applied to the prediction of vibration. Since multibody dynamics modeling method is a more practical and realistic modeling method in comparison with previous methods, it has the advantage of offering a virtual engineering environment.

(2) When the difference in stiffness between the isolators A and B is 200 %, the change in the tangential acceleration is less than 10 % in simulation and experiment. The radial acceleration also had little effect on experiment and simulation. Therefore, it can be concluded that the change in stiffness of the isolators has insignificant effects on acceleration.

(3) Increasing the radial acceleration and increasing the I_{zz} of the case in simulation decrease the acceleration about 20 %. But, it has little effects on the radial acceleration.

(4) The effect of increasing the mass of the weight balancer was different on the tangential acceleration and on radial acceleration. While the tangential acceleration decreased as the mass increased, the radial acceleration has the lowest values of 60 g by simulation and 80 g by experiment. Therefore, it could be observed that the optimum value of the weight balancer of this compressor is in the range of 60 g ~ 80 g.

(5) The tangential acceleration is excited to 60 % by compression and to 40 % by rotating parts. On the other hand, the radial acceleration is only excited by the rotating parts. Therefore, balancing of the rotating parts and other compression mechanism need to be controlled in order to control the tangential acceleration, and the radial acceleration can be controlled only by the rotating parts.

References

1. Padhy, S. K., "On the Dynamics of a Rotary Compressor: Part 1-Mathmatical Modeling. Advances in Design Automation," ASME, Vol. 1, pp. 207-217, 1993.
2. Padhy, S. K., "On the Dynamics of a Rotary Compressor: Part 2-Experimental Validation and Sensitivity Analysis. Advances in Design Automation," ASME, Vol. 1, pp. 219-227, 1993.
3. Yangisawa, T., Mori, M., Shimizu, T. and Ogi, T., "Vibration of a Rolling Piston Type Rotary Compressor," International Journal of Refrigeration, Vol. 7, No. 4, pp. 237-244, 1985.
4. Jeong, E. B., Hwang, S. W., Ahn, S. J. and Kim, J. K., "Vibration analysis of Rotary Compressor in Consideration of Ductility of Motor," Korean Society for Noise and Vibration Engineering, Collection of Learned Paper of 2002 Scientific Forum in Spring, pp. 1055-1060, 2002.
5. Haug, E. J., Computer Aided Kinematics and Dynamics of Mechanical System, Allyn and Bacon, USA, 1989.
6. www.lmsintl.com
7. www.adams.com
8. www.simpack.com
9. http://www.functionbay.com